Axial behavior of diffractive lenses under Gaussian illumination: complex-argument spectral analysis

Carlos J. Zapata-Rodríguez, Manuel Martínez-Corral, Pedro Andrés, and Amparo Pons

Department of Optics, University of Valencia, Dr. Moliner 50, E-46100 Burjassot, Spain

Received January 4, 1999; accepted April 5, 1999; revised manuscript received May 11, 1999

We present a general procedure to analyze the axial-irradiance distribution generated by an unlimited diffractive lens under coherent, Gaussian illumination. The resulting on-axis diffraction pattern, which is evaluated in terms of the power complex spectrum of the Fresnel-zone transmittance, explicitly depends on the truncation parameter that we define, which evaluates the effective number of zones illuminated by the Gaussian beam. Depending on the value of this parameter, different kinds of axial behavior are observed. In particular, for moderate values a multiple-focal-shift phenomenon appears, and a simple formula for its evaluation is presented. Additionally, for low values of the truncation parameter, a focal-merge effect is observed in multifocal zone plates. © 1999 Optical Society of America [S0740-3232(99)03209-3]

OCIS code: 220.2560.

1. INTRODUCTION

Zone plates have been widely used in optical systems[1] such as optical disk readout setups,[2] confocal scanning microscopes,[3,4] beam-shaping elements,[5] and miniature optical switching devices.[6] Advanced phototechnologies and computer synthesis of diffractive elements allow considerable facilitation of their fabrication and printing.[7] In contrast to designs using refractive elements, diffractive lenses provide important features uniquely suitable for such optical applications: (1) a zone plate is similar to a multifocal lens and has an infinity of foci, whose distances to the plate are a fraction of the principal focal length,[8] and (2) the dispersion resulting from a diffraction phenomenon is, in general, stronger than that from refraction, providing a more sensitive wavelength-to-focal-length dependence.[2,3] Most of the systems using diffractive lenses are laser technological setups, where the versatility and the small size of a fiber-based device make it an attractive candidate for a micromechanical optical arrangement.[9]

Several analytical descriptions have been proposed for the wave field in the focal regions of diffractive lenses under plane-wave illumination. Boivin[10] published an analytical study of the diffraction phenomenon produced by the Fresnel zone plate by summing up the contributions of each transparent zone. By using Fourier analysis, Novotný[11] interpreted the transmission function of diffractive lenses as a superposition of the transmission functions of ideal lenses. The three-dimensional wave-field structure in the focal region does not deviate from that of an ideal lens for a high number of periods.[12]

Diffractive lenses are featured by a limited numerical aperture that is constrained by the minimum size possible with current microfabrication technology. Eventually, this may lead to an optical device with a low number of periods. Interesting features are observed in the caustics of zone plates when the number of Fresnel zones is not large (<100). In the far field, an interference pattern of contrast nonlocalized fringes[5] has been observed that is due to the relevance of secondary diffraction orders. Koronkevich and Pal'chikova[13] have found that the field is asymmetric with respect to the nominal focal plane and that the maximum of intensity on the optic axis is shifted from the geometrical focus for zone plates with a stepwise kinoform phase profile. Jiang *et al.*[14] have found that the so-called focal-shift effect[15–17] also appears for a Fresnel zone plate under spherical uniform illumination, providing an approximated formula for the evaluation of the relative focal shift.

Boivin analysis[10] seems to be appropriate for diffractive lenses containing a low number of Fresnel zones. Otherwise, when the contribution of a large number of zones is significant, the Novotný[11] procedure yields results that are more efficient. However, for nonuniform illumination, it is possible to find a diffractive optical setup where a great number of Fresnel zones must be taken into account, though only a few of them contribute strongly to the overall irradiance distribution in the different focal regions.

The aim of this study is to present a novel formulation, which is highly efficient within a wide range of illumination considerations, for describing the axial behavior of diffractive lenses under Gaussian beam illumination. It is then straightforward to show that, under certain circumstances, it is possible to observe a focal-shift effect in zone plates of high number of periods, provided that the illumination has a nonuniform Gaussian profile. In fact, this assumption holds in laser technological setups where the light is emitted from a single-mode optical fiber. For this purpose, in Section 2 we develop an expression for the evaluation of the axial-irradiance distribution generated by an unlimited diffractive lens under Gaussian plane illumination. The resulting on-axis diffraction pattern explicitly depends on the truncation parameter defined here, which evaluates the effective number of Fresnel zones illuminated by the Gaussian beam. Section 3 shows that, depending on the value of this parameter, different kinds of axial behavior are observed. In particular, a multiple-focal-shift phenomenon appears for moderate values, and a simple formula for its evaluation is reported. To illustrate our formulation, Section 4 is devoted to investigating the axial behavior of several kinds of diffractive lenses. Specifically, the multiple-focal-shift effect for the cases of a Fresnel zone plate and a stepwise relief kinoform lens is theoretically discussed. In addition, interesting phenomena are found for under-unity truncation parameters, such as a merge of axial neighbor foci.

2. IRRADIANCE DISTRIBUTION ALONG THE OPTIC AXIS

Let us consider a circular diffractive lens that is fully illuminated by a plane Gaussian beam. For simplicity, we assume that the propagating wave impinges normally upon the diffractive lens in such a way that the center of the Gaussian pattern coincides with that of the zone plate (see Fig. 1). The amplitude transmission of such a diffractive plane element may be described by a periodic function with the square radial coordinate ρ^2 as

$$t(\rho) = \sum_{n=0}^{\infty} a\left(\frac{\rho^2}{T^2} - n\right) = a\left(\frac{\rho^2}{T^2}\right) \otimes \sum_{n=0}^{\infty} \delta(\rho^2 - nT^2), \tag{1}$$

where $\otimes$ represents the convolution operation and $a(\rho^2/T^2)$ stands for the transverse transmittance, usually denoted as the normalized unit cell, which is replicated with a period given by T^2. The wave-field distribution in the transverse plane just behind the zone plate, denoted from here on as the reference plane, can be expressed, according to the Kirchhoff boundary conditions,[18] as

$$U_0(\rho) = A \exp\left(-\frac{\rho^2}{\omega^2}\right) t(\rho), \tag{2}$$

where we have introduced a Gaussian attenuation along the radial coordinate that is due to the nonuniform distribution of the illuminating radiation. In Eq. (2) A indicates the incident-wave amplitude on the optic axis, and ω is the waist spot size. The diffracted field can be evaluated on a transverse plane with respect to the propagation direction, located a distance z from the reference plane, by means of the Fresnel–Kirchhoff diffraction formula (see Ref. 18, Sec. 4.2), that is,

$$U(r, z) = \frac{\exp(ikz)}{i\lambda z} \exp\left(i\frac{k}{2z}r^2\right) \int_0^{\infty} U_0(\rho) \times \exp\left(i\frac{k}{2z}\rho^2\right) J_0\left(2\pi\frac{r\rho}{\lambda z}\right) 2\pi\rho\, \mathrm{d}\rho. \tag{3}$$

The paraxial approximation that is assumed here will provide a suitable evaluation of the diffracted field when the inequality $z \gg T \gg \lambda$ holds, provided that the outermost Fresnel zones of the diffractive lens do not contribute significantly to the overall diffracted field.

By inserting Eq. (2) into Eq. (3), we can obtain the amplitude distribution along the optic axis by restricting the diffraction formula to the axial points $r = 0$. Moreover, it has been shown[19,20] that the resulting integral can be conveniently transformed with the use of a geometrical mapping given by $\zeta = \rho^2$. Therefore the axial-amplitude distribution may be expressed as

$$U(z) = A\frac{\pi}{\lambda z} \int_{-\infty}^{\infty} q(\zeta) \exp\left[i2\pi\left(\frac{1}{2\lambda z} + i\frac{1}{2\pi\omega^2}\right)\zeta\right] \mathrm{d}\zeta, \tag{4}$$

where we have neglected an unessential phase factor. We have introduced the function $q(\zeta) = t(\rho)$, which arises from the geometrical mapping performed in the diffraction integral, that is,

$$q(\zeta) = a\left(\frac{\zeta}{T^2}\right) \otimes \sum_{n=0}^{\infty} \delta(\zeta - nT^2). \tag{5}$$

Note that we have extended the lower limit of the integral in Eq. (4) to $-\infty$, since the function $q(\zeta)$ vanishes for $\zeta < 0$.

From Eq. (4) it is apparent that the axial behavior of a circular zone plate under Gaussian illumination is determined by the one-dimensional (1-D) Fourier transform, with complex scale factor, of the causal quasi-periodical function $q(\zeta)$. Then, profiting from the 1-D convolution nature of the function $q(\zeta)$, as shown in Eq. (5), we can rewrite the complex-argument Fourier transform of $q(\zeta)$ as a product of two terms. The first is simply the 1-D Fourier transform of the normalized unit cell, denoted as $\tilde{a}$, whereas the second is given by

$$\int_0^{\infty} \sum_{n=0}^{\infty} \delta(\zeta - nT^2) \exp\left[i2\pi\left(\frac{1}{2\lambda z} + i\frac{1}{2\pi\omega^2}\right)\zeta\right] \mathrm{d}\zeta = \sum_{n=0}^{\infty} \exp\left[i2\pi n\left(\frac{T^2}{2\lambda z} + i\frac{T^2}{2\pi\omega^2}\right)\right]. \tag{6}$$

Equation (6) represents a geometrical series of infinite terms. Fortunately, we can sum up all the terms by means of the well-known relation

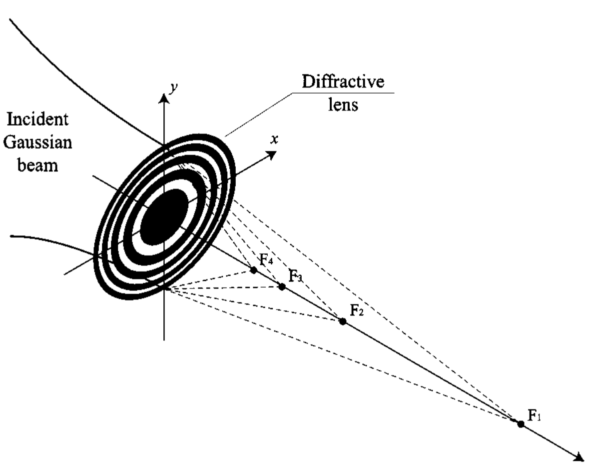

Fig. 1. Schematic diagram of the optical arrangement.

$$\sum_{n=0}^{\infty} x^n = \frac{1}{1-x}, \tag{7}$$

giving

$$F(N, \alpha) \equiv \frac{1}{1 - \exp\left[i 2\pi \left(\frac{N + i}{2\pi\alpha} \right) \right]}, \tag{8}$$

where the axial coordinate has been expressed in terms of

$$N = \pi \frac{\omega^2}{\lambda z}, \tag{9}$$

which stands for the Gaussian Fresnel number associated with the different diffraction patterns of the Gaussian beam,[21] and where we have introduced a new parameter, denoted as the truncation parameter, which we have defined as

$$\alpha = \frac{\omega^2}{T^2}. \tag{10}$$

This parameter indicates the number of Fresnel zones from the diffractive lens that are covered by the Gaussian waist spot. Therefore it gives a rough estimation of the number of Fresnel zones that effectively contribute to the diffraction pattern.

Finally, the axial-irradiance distribution can properly be written, apart from a constant factor A^2, as

$$I(N) = \left(\frac{N}{\alpha} \right)^2 \left| \tilde{a}\left(\frac{N + i}{2\pi\alpha} \right) \right|^2 |F(N, \alpha)|^2, \tag{11a}$$

where the term $|F(N, \alpha)|^2$ can be expressed as[22]

$$|F(N, \alpha)|^2 = \frac{1}{4} \frac{\exp(1/\alpha)}{\sin^2(N/2\alpha) + \sinh^2(1/2\alpha)}. \tag{11b}$$

This relevant formula, which fully describes the axial behavior of diffractive lenses for any value of the truncation parameter, indicates that the axial-irradiance distribution is governed by the product of three different factors. The first, $(N/\alpha)^2$, describes the irradiance attenuation inherent in spherical wave propagation. The second term, defined here as the diffraction term, takes into account the diffraction effect produced by the amplitude transmittance of the unit cell. Finally, the third term, or interference term, considers the focusing properties of a zone plate under Gaussian illumination.

3. FOCI GENERATION AND THE MULTIPLE-FOCAL-SHIFT EFFECT

To investigate the focusing properties associated with a diffractive lens, in Fig. 2 we represent graphically the interference term $|F|^2$ versus a normalized Gaussian Fresnel number $N/2\pi\alpha$ for some typical values of the truncation parameter α. From this figure it is apparent that the interference term is composed of an infinite number of uniformly distributed peaks, whose maxima are located accordingly for Gaussian Fresnel numbers, taking the values

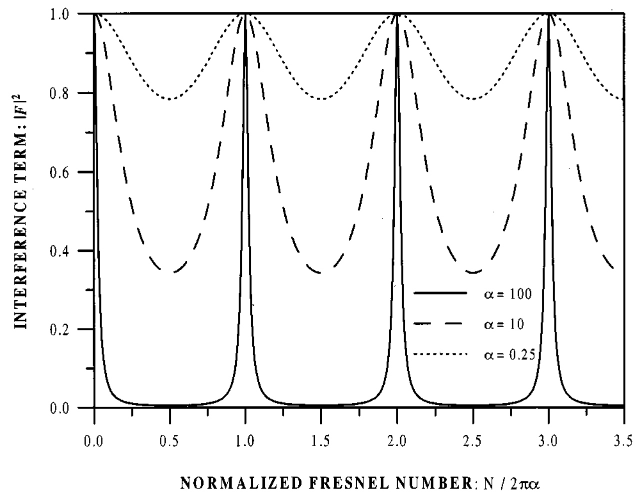

Fig. 2. Normalized interference term versus reduced axial coordinate $N/2\pi\alpha$ for different values of the truncation parameter α. The peak structures of this term quickly disappear for decreasing values of the truncation parameter close to unity.

$$N_n = 2\pi n\alpha \qquad \text{with } n = 0, \pm 1, \pm 2, \ldots. \tag{12}$$

The axial positions of the local maxima expressed in terms of the axial coordinate z are $f_n = T^2/2\lambda n$, which precisely coincide with the well-known foci positions of a circular zone plate.[8] For $n = 0$ we find the singularity $f_0 \to \infty$, whose interpretation is that the curvature of the zero-order diffracted beam is flat. We observe that the width of the interference-term peaks depends only on the truncation parameter α.

In analogy to the resonance-properties analysis of a Fabry–Perot interferometer,[23] we can evaluate the ratio of the gap hold between two adjacent peaks to the peak width, giving the so-called finesse that is,

$$\mathcal{F} = \frac{\pi}{2} \frac{1}{\sinh(1/2\alpha)}. \tag{13}$$

The analogy is fully justified in the sense that a multiple-wave interference process occurs, one concerning an infinite number of plane waves generated in a resonant cavity and the other involving Fresnel wavelets proceeding from the multiple zones of the diffracting plate.

Standard use of diffractive lenses requires a high number of Fresnel zones to be well illuminated, which is established mathematically as α becomes much higher than unity. This results in an approximately linear dependence of $\mathcal{F}$ on the truncation parameter, i.e., $\mathcal{F} = \pi\alpha$. In this case the interference term contains a set of well-defined peaks with a low focal depth (see Fig. 2). In these small regions, the propagation factor and the diffracting term, contributing to the axial-irradiance pattern [see Eq. (11a)], do not vary appreciably, taking the approximate values $(2\pi n)^2$ and $|\tilde{a}(n)|^2$, respectively. This agrees with the commonly used assumption[24] that the height of the nth-order focus of a diffractive lens is directly proportional to the product $n^2|\tilde{a}(n)|^2$.

Nevertheless, the above analysis no longer holds for low values of the truncation parameter. Most of the practical uses of diffractive lenses in current micro-optical setups satisfy such a constraint.[1] According to Eq. (13), in this case the parameter $\mathcal{F}$ comes closer to unity, that is, the width of every peak increases with respect to the separation with the neighboring peaks, starting an overlapping process. Simultaneously, both the propagation factor and the diffraction term may notably change in the focal regions. For the sake of simplicity, we will assume that the major deviation is caused by the propagation factor, which holds for moderate values of α, and the most typical unit-cell profiles a. Then we can expand the denominator in Eq. (8) into a Taylor series, up to a first-order approximation, about the nth-order peak, giving

$$F_n(N, \alpha) = \frac{i}{2\pi[(N - N_n) + i]/(2\pi\alpha)}. \tag{14}$$

If we approximate the interference term to the constant value $|\tilde{a}(n)|^2$, the axial behavior in the vicinities of the nth zone-plate focus may be written in accordance with Eq. (11a) as

$$I_n(N) = |\tilde{a}(n)|^2 \frac{N^2}{(N - N_n)^2 + 1}. \tag{15}$$

According to Eq. (15), we find that the loci of the local maxima in the axial-irradiance distribution are given by

$$N_{\max}(n) = N_n\left(1 + \frac{1}{{N_n}^2}\right) = N_n\left[1 + \frac{1}{(2\pi n\alpha)^2}\right]. \tag{16}$$

From this equation we confirm that when the truncation parameter α, and then N_n, tend to infinity, the maxima along the axial-irradiance distribution coincide with the foci of the zone plate. However, for decreasing values of α, the local maxima suffer a slight displacement given by higher values of the Gaussian Fresnel number, that is, toward the diffractive lens. This interesting result allows us to recognize the existence of a multiple-focal-shift effect in zone plates under Gaussian illumination for moderate values of the truncation parameter.

Note that Eq. (15) is similar to that describing the axial behavior of a spherical Gaussian beam.[25] Interestingly, this occurs when a kinoform lens is illuminated by a plane Gaussian beam. In this case the unit-cell profile can be expressed as

$$a(\xi) = \exp(-i2\pi m\xi), \tag{17}$$

where m is an integer. Specifically, $m = 1$ corresponds to a converging diffractive lens, $m = -1$ represents a diverging kinoform zone plate, and the harmonic diffractive lenses[26] hold for $m = \pm 2, \pm 3, \ldots$. The diffracting term can be analytically evaluated in terms of the sinc function, i.e.,

$$\mathrm{sinc}(x) = \frac{\sin(\pi x)}{\pi x}, \tag{18}$$

so, finally, we have

$$\left|a\left(\frac{N + i}{2\pi\alpha}\right)\right|^2 = \left|\mathrm{sinc}\left(\frac{N + i}{2\pi\alpha} - m\right)\right|^2 = \frac{(2\alpha)^2}{\exp(1/\alpha)} \frac{\sin^2(N/2\alpha) + \sinh^2(1/2\alpha)}{(N - N_m)^2 + 1}. \tag{19}$$

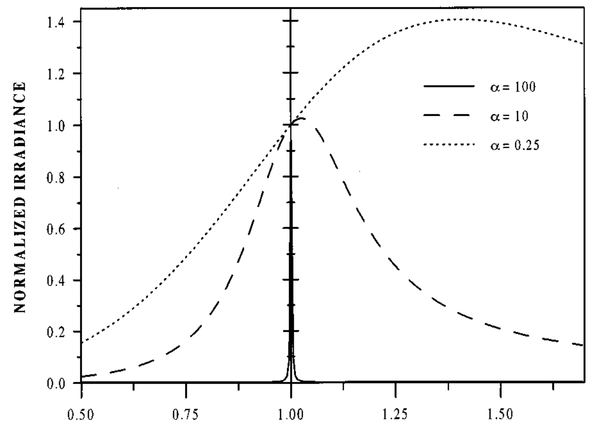

Fig. 3. Axial-irradiance distribution, normalized to the in-focus value, corresponding to a converging kinoform zone plate ($m = 1$) illuminated by a Gaussian beam. We observe a focal-shift effect when the truncation parameter decreases to values close to unity. In this case the point of maximum irradiance along the axis has a Gaussian Fresnel number higher than that corresponding to the principal focus, meaning that the focus shifts toward the kinoform lens.

By inserting Eq. (19) into Eq. (11a), we find that the irradiance distribution along the optic axis is given by

$$I(N) = \frac{N^2}{(N - N_m)^2 + 1}. \tag{20}$$

We can observe that Eqs. (15) and (20) follow the same behavior when the mth order is evaluated, that is, $n = m$. Figure 3 shows the axial-irradiance distribution of such a phase plate in terms of the reduced coordinate $N/N_m = N/2\pi m\alpha$ for different values of the truncation parameter. We clearly observe a focal-shift effect for values of α close to and lower than unity.

4. PARTICULAR EXAMPLES: FOCI-MERGE EFFECT

Next, we apply our formalism to the well-known Fresnel zone plate. This binary diffractive element consists of a set of concentric transparent and obscured annuli, all having the same area and distributed alternately along the transverse direction.[24] The unit cell is then given by

$$a(\xi) = \begin{cases} 1 & 0 \leqslant \xi < 1/2 \\ 0 & \text{otherwise} \end{cases}. \tag{21}$$

The Fourier transform can be easily expressed in terms of the sinc function, giving

$$\tilde{a}(u) = \frac{1}{2}\exp\left(i\frac{\pi}{2}u\right)\mathrm{sinc}\left(\frac{u}{2}\right). \tag{22}$$

Now we can determine the axial behavior by using Eqs. (11), so the irradiance distribution along the axis is given by

$$I(N) = \exp(1/2\alpha)\frac{N^2}{1+N^2}\frac{\sin^2(N/4\alpha) + \sinh^2(1/4\alpha)}{\sin^2(N/2\alpha) + \sinh^2(1/2\alpha)}. \tag{23}$$

In Fig. 4 we observe the predicted multiple-focal-shift effect. For high values of the truncation parameter, the height of the maxima along the axis equalizes, as predicted for uniform plane illumination by standard procedures.[24] For decreasing values of the truncation parameter α close to unity, the width of the peaks constituting the multifocal structure increases. This effect, which appears by virtue of the interference term as discussed in Section 3, is accompanied by a stronger influence of the asymmetry characterizing the propagation term. Although both combined effects yield a multiple focal shift, this effect is almost negligible except for the principal focus. Finally, the diffraction term selects the height of the axial peaks, which explains why even orders vanish.

In Fig. 5 we check the accuracy of Eq. (16) for evaluating the amount of focal shift suffered by the first three foci. It is shown that Eq. (16) gives suitable values for the focal shift for $\alpha \geqslant 1$. In this case the displacements of the maxima are always lower than the distance between adjacent peaks. Otherwise, the approximated formula given in Eq. (16) overestimates the multiple focal shift. In this case the diffractive term must be taken into account, since the assumption of a slow dependence on the Gaussian Fresnel number within the focal region holds only for values of the truncation parameter not lower than unity. Interestingly, we observe that for $\alpha = 0.17$ ($1/\alpha = 5.8$ in the plot abscissa) the principal focus suffers a rapid merge process with the third-order maximum. For lower values of α, we find several successive points where higher-order foci merge, giving rise to a monotonic behavior of the axial-irradiance distribution. For the sake of clarity, in Fig. 6 we illustrate graphically the influence of the focal-merge effect on the axial-irradiance distribution for low values of the truncation parameter α.

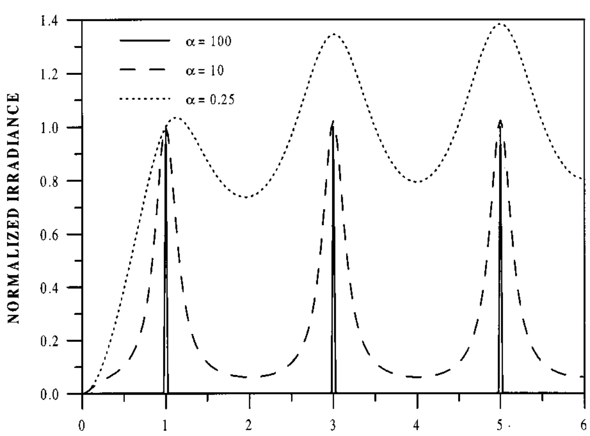

Fig. 4. Normalized axial-irradiance distribution versus reduced Gaussian Fresnel number. We observe a deviation from the multifocal behavior for truncation parameters close to unity. The height of the peaks does not equalize, since the propagation factor causes an asymmetry along the optic axis. Also, this term leads to the displacement of the axial maxima toward the Fresnel zone plate, giving rise to a multiple focal shift.

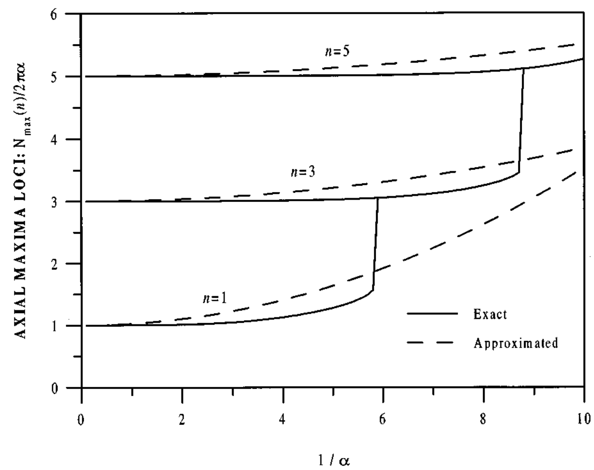

Fig. 5. Graphical representation of the axial maxima positions for the first three diffracting orders in terms of the truncation parameter. We represent the approximated expression given in Eq. (16) by dashed curves.

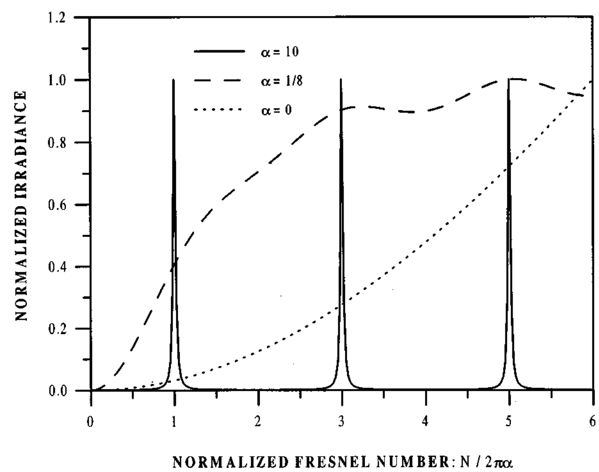

Fig. 6. Axial-irradiance distribution versus normalized Fresnel number of a Fresnel zone plate illuminated with a plane Gaussian beam for values of $\alpha = 10$, where we clearly observe focal-peak generation, $\alpha = 1/8$, where the first- and third-order maxima merge, and $\alpha = 0$, corresponding to an ideally nontruncated Gaussian beam. For convenience, the normalization of the axial-irradiance distribution is different for the cases presented here.

To end up, we analyze the axial response of phase diffractive lenses with a stepwise profile, i.e., diffractive elements that approach a kinoform lens by the introduction of a phase-step relief.[12] Recent technological procedures[1] allow the use of steps with a small phase shift and reduced lateral dimensions, implying that the phase-plate efficiency can be extremely high. Then we describe the unit cell of such a structure as

$$a(\xi) = \exp[-i2\pi\phi(\xi)], \tag{24}$$

where

$$\phi(\xi) = \begin{cases} 0 & 0 \leqslant \xi < 1/M \\ 1/M & 1/M \leqslant \xi < 2/M \\ 2/M & 2/M \leqslant \xi < 3/M \\ \vdots & \vdots \\ (M-1)/M, & (M-1)/M \leqslant \xi \leqslant 1 \end{cases}. \quad (25)$$

In Eq. (25) M stands for the number of steps used in the kinoform phase-profile approach. The spectrum of the unit cell given in Eq. (24) can be written as

$$\tilde{a}(u) = \int_0^1 a(\zeta)\exp(i2\pi u\zeta)\mathrm{d}\zeta$$
$$= \sum_{n=0}^{M-1} \exp\left(-i2\pi\frac{n}{M}\right)\int_{n/M}^{(n+1)/M}\exp(i2\pi u\zeta_n)\mathrm{d}\zeta_n . \quad (26)$$

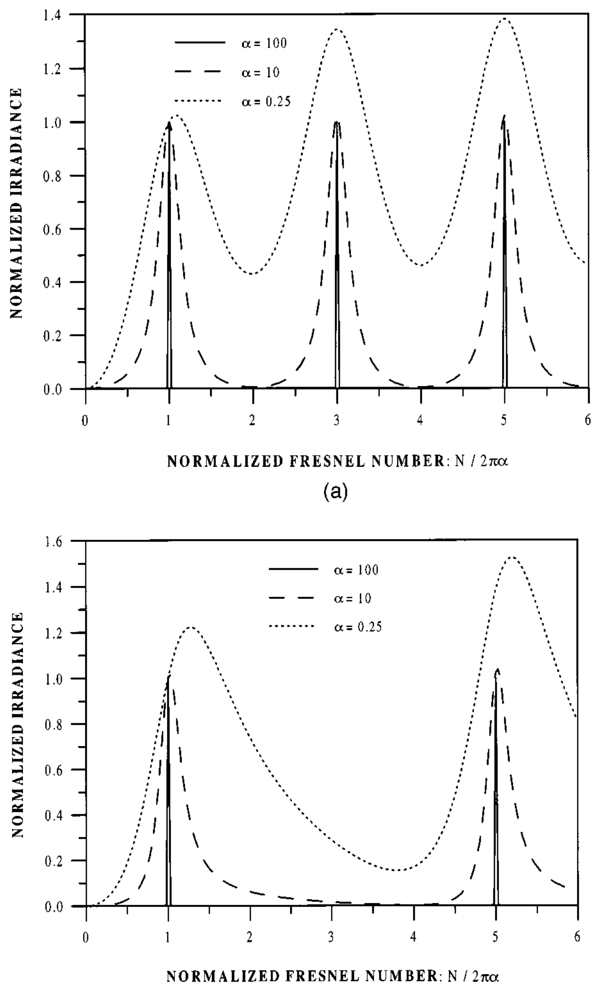

Fig. 7. Normalized axial-irradiance distribution for a kinoform zone plate with a stepwise profile. We have selected (a) $M = 2$ and (b) $M = 4$ phase steps as examples. We observe that for increasing number of steps, successive diffracting orders vanish. Thus, for the limiting case of an infinite number of steps, we generate a single-focus diffractive lens.

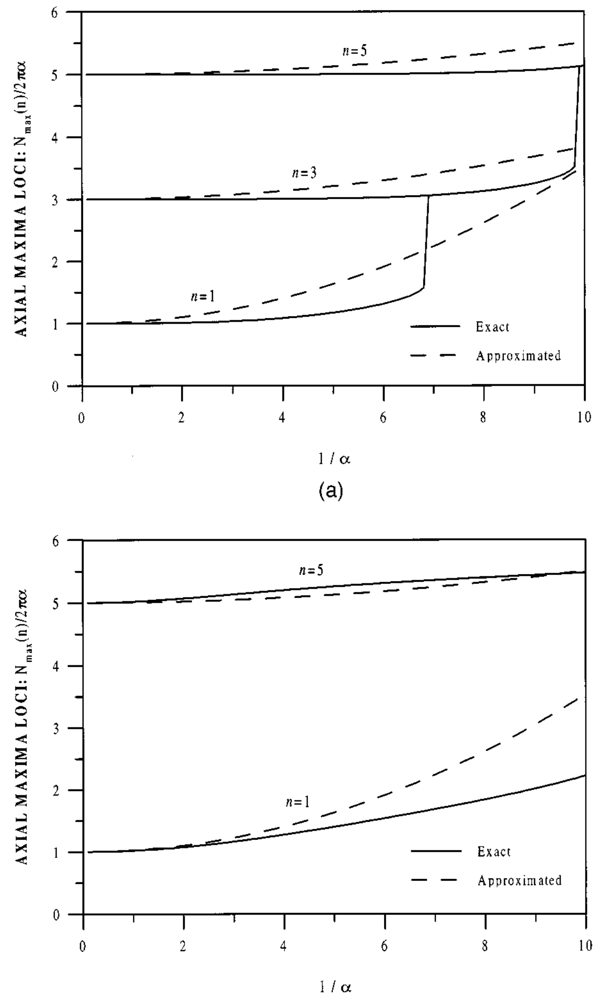

Fig. 8. Position of the maxima corresponding to the axial-irradiance distribution in terms of the truncation parameter. The geometrical parameters of the stepwise relief diffractive lens coincide with those of Fig. 7.

By an appropriate change of variable within each integration in Eq. (26), i.e., $\zeta_n' = \zeta_n - n/M$, we evaluate the 1-D Fourier transform of the unit cell as

$$\tilde{a}(u) = \left[\sum_{n=0}^{M-1}\exp\left(-i2\pi\frac{n}{M}\right)\exp\left(i2\pi\frac{n}{M}u\right)\right] \times \int_0^{1/M}\exp(i2\pi u\zeta)\mathrm{d}\zeta. \quad (27)$$

The integral can be expressed in terms of the sinc function [see Eq. (18)], whereas the finite sum is analytically described by using Eq. (7), so that we finally obtain

$$\tilde{a}(u) = \exp\left(i\frac{\pi}{M}\right)\exp[i\pi(u-1)] \times \frac{\mathrm{sinc}(u-1)}{\mathrm{sinc}[(u-1)/M]}\mathrm{sinc}(u/M). \quad (28)$$

Finally, Eqs. (11) provide the axial-irradiance distribution of a stepwise phase diffractive lens, giving

$$I(N) = \frac{N^2}{1 + N^2} \frac{\sin^2(N/2M\alpha) + \sinh^2(1/2M\alpha)}{\sin^2(N/2M\alpha - \pi/M) + \sinh^2(1/2M\alpha)}. \tag{29}$$

Figure 7 shows graphically the axial behavior expressed in Eq. (29) for a zone plate with (a) a two-step ($M = 2$) and (b) a four-step ($M = 4$) phase relief. We observe that the number of foci decreases with the number of phase steps M. The distance between adjacent foci is then enlarged following a $2\pi M\alpha$ rule, given in terms of the Gaussian Fresnel number.[13] Consequently, the influence of adjacent foci diminishes, and for a low truncation parameter α the interference term in Eq. (11b) still becomes significant in the multifocal structure. Moreover, the axial behavior shows a higher resistance to the focal-merge effect, and Eq. (16) reflects a more realistic distribution of the foci locations, as shown in Fig. 8.

5. SUMMARY AND CONCLUSION

We have analyzed the axial-irradiance distribution of ideal diffractive lenses illuminated by a plane nonuniform Gaussian beam. The axial behavior can be evaluated by means of a simple formalism based on a complex-argument spectral procedure. We have proved that the resulting distribution is composed of three different terms: one is associated with the diffraction effects of the unit cell, another concerns the interference process caused by the multiple zone structure of a diffractive lens, and the last considers the attenuation inherent in wave propagation.

Within this closed-form formalism, we can interpret the multiple-foci generation associated with a zone plate, as well as a multiple-focal-shift phenomenon observed when the effective number of illuminated zones, defined here as the truncation parameter, is close to unity. Finally, with the aid of some particular examples, a focal-merge effect is shown as a transition to an axial monotonic behavior for very low values of the truncation parameter. It is worthy to mention that, in dual-focus systems, the propagation factor can not only shift the focal loci but also produce a focal switch toward the diffracting element.[27,28]

ACKNOWLEDGMENTS

Carlos J. Zapata-Rodríguez gratefully acknowledges financial support from the Dirección de Investigación Científica y Enseñanza Superior, Ministerio de Educación y Ciencia, Spain.

Address correspondence to Carlos J. Zapata-Rodríquez at the location on the title page or by e-mail, carlos.zapata@uv.es.

REFERENCES AND NOTES

1. Feature issue on diffractive optics applications, Appl. Opt. **34**, 2399–2559 (1995).
2. Y. Ono and N. Nishida, "Holographic laser scanners using generalized zone plates," Appl. Opt. **21**, 4542–4548 (1982).
3. S. L. Dobson, P.-C. Sun, and Y. Fainman, "Diffractive lenses for chromatic confocal imaging," Appl. Opt. **36**, 4744–4748 (1997).
4. P. C. Lin, P.-C. Sun, L. Zhu, and Y. Fainman, "Single-shot depth-section imaging through chromatic slit-scan confocal microscopy," Appl. Opt. **37**, 6764–6770 (1998).
5. M. Rossi and T. Hesser, "Interference effects in diffractive beam shaping elements," in *Diffractive Optics and Micro-Optics*, Vol. 10 of 1998 OSA Technical Digest Series (Optical Society of America, Washington, D.C., 1998), paper DMD3-1.
6. D. G. Greywall, "A micromechanical optical switch with a zone-plate reflector," J. Phys. D **30**, 2191–2208 (1987).
7. V. P. Koronkevich, V. P. Kiriyanov, F. I. Kokoulin, I. G. Palchikova, A. G. Poleshchuk, A. G. Sedukhin, E. G. Churin, A. M. Shcherbachenko, and Y. I. Yurlov, "Fabrication of kinoform optical elements," Optik (Stuttgart) **67**, 257–266 (1984).
8. V. Moreno, J. F. Román, and J. R. Salgueiro, "High efficiency diffractive lenses: deduction of kinoform profile," Am. J. Phys. **65**, 556–562 (1997).
9. D. L. Dichensheets and G. S. Kino, "Micromachined scanning confocal microscope," Opt. Lett. **21**, 764–766 (1996).
10. A. Boivin, "On the theory of diffraction by concentric arrays of ring-shaped apertures," J. Opt. Soc. Am. **42**, 60–64 (1952).
11. M. Novotný, "A new series representation of the Fresnel diffraction field of axially symmetrical filters," Opt. Acta **24**, 551–565 (1977).
12. R. Chmelik, "Analytic description of wave fields in focal regions of diffractive lenses," J. Mod. Opt. **43**, 1463–1471 (1996).
13. V. P. Koronkevich and I. G. Pal'chikova, "Modern zone plates," Optoelectron. Instrum. Data Process. **1**, 86–100 (1992).
14. X. Jiang, S. Wang, E. Bernabeu, and J. Alda, "ABCD matrix and focal shift for Fresnel zone plates," Optik (Stuttgart) **95**, 16–18 (1993).
15. Y. Li and E. Wolf, "Focal shifts in diffracted converging spherical waves," Opt. Commun. **39**, 211–215 (1981).
16. M. Martínez-Corral, C. J. Zapata-Rodríguez, P. Andrés, and E. Silvestre, "Effective Fresnel-number concept for evaluating the relative focal shift in focused beams," J. Opt. Soc. Am. A **15**, 449–455 (1998).
17. S. De Nicola, D. Anderson, and M. Lisak, "Focal shift effects in diffracted focused beams," Pure Appl. Opt. **7**, 1249–1259 (1998).
18. J. W. Goodman, *Introduction to Fourier Optics* (McGraw-Hill, San Francisco, 1996), Sec. 3.4.2.
19. C. W. McCutchen, "Generalized aperture and three-dimensional diffraction image," J. Opt. Soc. Am. **54**, 240–244 (1964).
20. M. Martínez-Corral, P. Andrés, and J. Ojeda-Castañeda, "On-axis diffractional behavior of two-dimensional pupils," Appl. Opt. **33**, 2223–2229 (1994).
21. S. Wang, E. Bernabeu, and J. Alda, "Unified and generalized Fresnel numbers," Opt. Quantum Electron. **24**, 1351–1358 (1992).
22. Hint: $|\sin(x + iy)|^2 = \sin^2(x) + \sinh^2(y)$.
23. P. W. Milonni and J. H. Eberly, *Lasers* (Wiley, New York, 1988), Chap. 11.
24. A. R. Shulman, *Optical Data Processing* (Wiley, New York, 1970), Chap. 9.
25. W. H. Carter, "Focal shift and concept of effective Fresnel number for a Gaussian laser beam," Appl. Opt. **21**, 1989–1994 (1982).
26. D. W. Sweeney and G. E. Sommargren, "Harmonic diffractive lenses," Appl. Opt. **34**, 2469–2475 (1995).
27. Y. Li, "Focal shift and focal switch in dual-focus systems," J. Opt. Soc. Am. A **14**, 1297–1304 (1997).
28. M. Martínez-Corral and V. Climent, "Focal switch: a new effect in low-Fresnel-number systems," Appl. Opt. **35**, 24–27 (1996).